JSCAI

Original Research

Efficacy of Coronary Calcium Score in Predicting Coronary Artery Morphology in Patients With Obstructive Coronary Artery Disease

Xingwei He, MD [a,b,†], Soe Maung, MBChB [a,†], Anantharaman Ramasamy, MBChB, PhD [a,c],
Mohamed O. Mohamed, PhD [a,d], Retesh Bajaj, MBChB [a,c],
Nathan Angelo Lecaros Yap, MBChB [a], Medeni Karaduman, MD [e],
Yaojun Zhang, MD, PhD [f], Pieter Kitslaar, MSc [g,h], Alexander Broersen, PhD [h],
Johan H.C. Reiber, PhD [g,h], Jouke Dijkstra, PhD [h], Patrick W. Serruys, MD, PhD [i,j],
James C. Moon, MD [a,k], Andreas Baumbach, MD, PhD [a,c], Ryo Torii, MSc, PhD [l],
Francesca Pugliese, MD, PhD [a,c], Christos V. Bourantas, MD, PhD [a,c,*]

[a] Department of Cardiology, Barts Heart Centre, Barts Health NHS Trust, London, United Kingdom; [b] Division of Cardiology, Department of Internal Medicine, Tongji Hospital, Tongji Medical College, Huazhong University of Science and Technology, Wuhan, China; [c] Centre for Cardiovascular Medicine and Devices, William Harvey Research Institute, Queen Mary University of London, London, United Kingdom; [d] Institute of Health Informatics, University College London, London, United Kingdom; [e] Department of Cardiology, Faculty of Medicine, Yuzuncu Yil University Van, Van, Turkey; [f] Department of Cardiology, Xuzhou Third People's Hospital, Xuzhou, China; [g] Division of Image Processing, Department of Radiology, Leiden University Medical Center, Leiden, the Netherlands; [h] Medis Medical Imaging Systems, Leiden, the Netherlands; [i] Faculty of Medicine, National Heart & Lung Institute, Imperial College London, London, United Kingdom; [j] Department of Cardiology, University of Galway, Galway, Ireland; [k] Institute of Cardiovascular Sciences, University College London, London, United Kingdom; [l] Department of Mechanical Engineering, University College London, London, United Kingdom

ABSTRACT

Background: Coronary artery calcium score (CACS) is an established marker of coronary artery disease (CAD) and has been extensively used to stratify risk in asymptomatic individuals. However, the value of CACS in predicting plaque morphology in patients with advanced CAD is less established. The present analysis aims to assess the association between CACS and plaque characteristics detected by near-infrared spectroscopy-intravascular ultrasound (NIRS-IVUS) imaging in patients with obstructive CAD.

Methods: Seventy patients with obstructive CAD underwent coronary computed tomography angiography (CTA) and 3-vessel NIRS-IVUS imaging were included in the present analysis. The CTA data were used to measure the CACS in the entire coronary tree and the segments assessed by NIRS-IVUS, and these estimations were associated with the NIRS-IVUS measurements at a patient and segment level.

Results: In total, 65 patients (188 segments) completed the study protocol and were included in the analysis. A weak correlation was noted between the CACS, percent atheroma volume (r = 0.271, P = .002), and the calcific burden measured by NIRS-IVUS (r = 0.648, P < .001) at patient-level analysis. Conversely, there was no association between the CACS and the lipid content, or the incidence of high-risk plaques detected by NIRS. Linear regression analysis at the segment level demonstrated an association between the CACS and the total atheroma volume (coefficient, 0.087; 95% CI, 0.024-0.149; P = .008) and the calcific burden (coefficient, 0.117; 95% CI, 0.048-0.186; P = .001), but there was no association between the lipid content or the incidence of high-risk lesions.

Conclusions: In patients with obstructive CAD, the CACS is not associated with the lipid content or plaque phenotypes. These findings indicate that the CACS may have a limited value for screening or stratifying cardiovascular risk in symptomatic patients with a high probability of CAD.

Introduction

Coronary artery calcium score (CACS) assessment provides useful prognostic information and enables the identification of patients at risk of suffering cardiovascular events. Cumulative data have shown that an increased CACS is a marker of coronary atherosclerosis and is associated with a high event rate in asymptomatic patients with no previous cardiac history.[1–4] Therefore, today CACS has IIb recommendation in the European Society of Cardiology guidelines for primary prevention for risk stratification and modifying treatment.[5] However, in patients with advanced disease, the value of the CACS is less well established. A meta-analysis of the MESA study has demonstrated no difference in the incidence of hard clinical end points (death resuscitated cardiac arrest or myocardial infarction) in patients with high (400-999) and very high (≥1000) CACS indicating that this tool may have a limited value in identifying vulnerable patients among those with advanced coronary artery disease (CAD).[6] These findings were not supported, however, by most recent reports including an analysis of the MESA study, where the patients had a longer follow-up, showing that a very high CACS provides useful prognostic information and is associated with worse prognosis compared to a high CACS.[7–10]

In an attempt to shed light on the value of CACS in assessing coronary artery phenotypes and predicting outcomes, a post hoc analysis of the SCOT-Heart study examined the association between CACS and plaque characteristics in patients with chest pain and demonstrated that high-risk plaque characteristics detected by coronary computed tomography angiography (CTA) increase between patients with 0, minimal (1-9) and low (10-99) CACS but did not increase further in patients with moderate (100-399), high (400-999) and very high (≥1000) CACS.[11] Intravascular imaging studies assessing the performance of CACS in evaluating plaque morphology have provided contradictory results with some studies showing a strong association and others no correlation between CACS and the lipid component.[12–14] The present study aims to provide additional insights into the value of the CACS in predicting plaque morphology and examines in a large number of patients with advanced CAD, the association between CACS and plaque characteristics detected by near-infrared spectroscopy-intravascular ultrasound (NIRS-IVUS).

Methods

Study population

This is a post hoc analysis of a recently conducted study that aimed to examine the safety and efficacy of CTA in assessing coronary artery morphology and physiology using NIRS-IVUS as a reference standard (ClinicalTrials.gov; NCT03556644).[15] The study included 70 patients with chronic coronary syndrome who had an invasive coronary angiogram demonstrating obstructive CAD which required either further assessment or treatment with percutaneous coronary intervention (PCI). All patients underwent CTA before being listed for repeat coronary angiography, PCI (if needed), and 3-vessel NIRS-IVUS imaging. The study was conducted in line with the Declaration of Helsinki and approved by the local ethics committee (REC reference: 17/SC/0566). All participants provided written informed consent before study enrolment.

CTA data acquisition

Coronary computed tomography angiography was performed using a third-generation dual-source computed tomography (CT) scanner (SOMATOM Force, Siemens Healthineers). Before CTA, participants received sublingual nitroglycerin (400 µg), and intravenous metoprolol (maximum 40 mg), when their heart rate was >70 beats per minute, provided there was no contraindication. Scan parameters included prospective ECG-triggered sequential scan mode, gantry rotation time of 250 ms, 128 × 2 × 0.5 mm, collimation with z-flying focal spot for both detectors, and a minimum tube voltage of 100 kV defined by the CarekV algorithm, whereas the tube current was determined by the scanner. In this study, noncontrast CT imaging was not performed so as to minimize additional radiation.

NIRS-IVUS data acquisition

NIRS-IVUS imaging was performed in all the recruited patients before PCI in their 3 major epicardial vessels and large side branches (diameter ≥2 mm) using a 2.4F Makoto NIRS-IVUS 35-65 MHz Imaging System (Infraredx). The probe was advanced to the distal end of the vessel and then was withdrawn using an automated pull-back device at a speed of 0.5 mm/s. If an obstructive lesion prohibited the advancement of the NIRS-IVUS probe, then this was predilated before NIRS-IVUS imaging with a 2-mm balloon.

NIRS-IVUS and CTA data analysis and coregistration

Coronary computed tomography angiography analysis was performed using commercially available CT plaque analysis software (QAngioCT Research Edition 3.1, Medis Medical Imaging Systems). The coronary tree was extracted and the most proximal and distal side branches that were visible on both CTA and NIRS-IVUS were identified and used to define a segment of interest—ie, the coronary segment that was assessed by both modalities. Stented segments, segments with poor image quality, and those with significant artifacts were excluded from the analysis.

The NIRS-IVUS data corresponding to the segment of interest were analyzed, by an expert analyst with an established reproducibility, blinded to the CTA images.[16] First the NIRS-IVUS end-diastolic frames were automatically extracted using an in-house deep learning methodology and then in these frames the lumen and external elastic membrane (EEM) borders were detected.[17] In addition, the circumferential distribution of the calcific tissue was manually annotated with an arc and these annotations together with the lipid core distribution, derived from NIRS, were used to generate a 2-dimensional (2D) color-coded map displaying the lipid core in yellow, and calcium in semitransparent white with the X-axis indicating the longitudinal and the Y-axis the circumferential location of the different plaque components.

Coronary artery calcium score computation was performed using a previously described method designed to estimate the CAC in contract CT that has been incorporated in an in-house customized research version of CalcScore software (V1.1.1 by Medis Specials bv, Figure 1). Axial planes that were 3 mm apart were defined and in these, the coronary calcium was automatically detected as the areas in the coronary arteries that had a minimum Hounsfield Unit (HU) threshold above that of the lumen HU values, so as to differentiate calcific tissue from the lumen volume, and an area >1 mm^2, which is the reference value in conventional calcium scoring analysis.[18] In this study we did not use a prespecified HU cutoff to define the presence of calcium but a patient-specific cutoff as there is a discrepancy in the literature about the optimal HU cutoff for detecting calcification in CTA.[19–23] To ensure accurate and reproducible detection of coronary calcification, the analyst was able to inspect during this process the multiplanar curve reconstructed CTA images, identify in these the presence of coronary calcification, and ensure that the selected HU cutoff in the CalcScore software allowed detection of coronary calcification in axial planes. The analysis was performed by an operator (C.V.B.) with 6 years of experience in CTA analysis for each segment of interest assessed by NIRS-IVUS and for the entire coronary artery tree. Stented segments were excluded from the CACS computation.
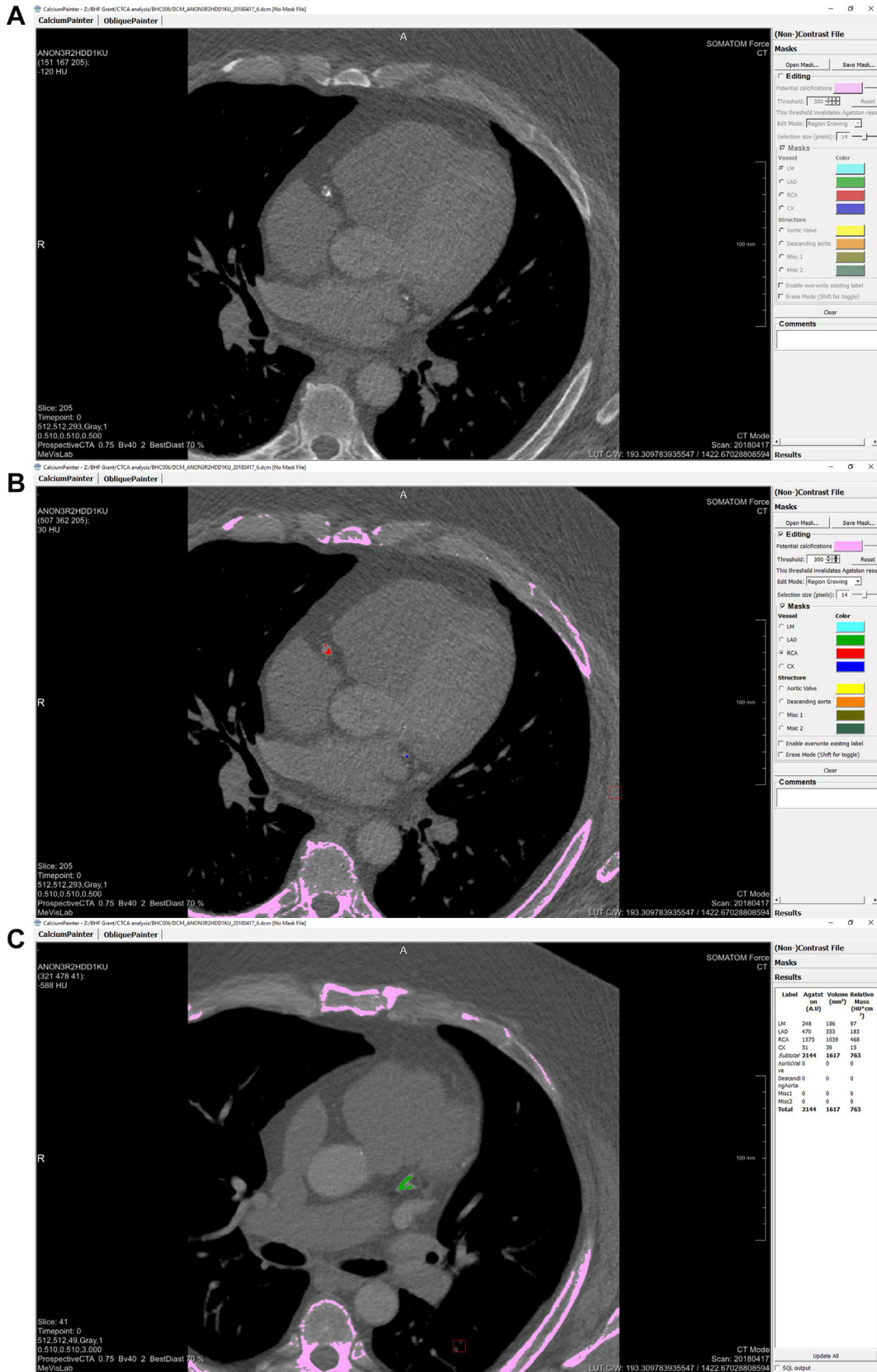
Figure 1.
Snapshots of the CalcScore software used for the coronary artery calcium score (CACS) computation. Panel (**A**) illustrates an axial CT plane where the analyst can identify the presence of coronary calcification and apply the 'optimal HU cutoff that allows automated detection of calcific tissue. The estimations of the algorithm are displayed in panel (**B**), and depending on the vessel, are shown in different colors (red for the RCA, green for the LAD, and blue for the LCx). After the automated detection of the calcific tissue, the CACS is computed for each coronary artery and for the entire coronary tree (**C**). LAD, left anterior descending artery; LCx, left circumflex coronary artery; RCA, right coronary artery.

The interobserver variability of the analyst was tested in a set of 25 patients against the estimations of a second operator; in this set, the analysis was repeated twice to also test the expert's intraobserver variability. Analysts' variability was tested using the intraclass correlation coefficient (ICC).

Association of CACS and plaque characteristics

The association between CACS and plaque characteristics was examined at segment- and patient-levels.

Segment-level analysis. The lumen and EEM borders detected in NIRS-IVUS images were used to compute the lumen, EEM, total atheroma volume (TAV, defined as EEM – lumen volume), and percent atheroma volume (PAV, defined as $100 \times$ TAV divided by the EEM volume). In addition, the maps of plaque distribution were used to compute the lipid core burden index (LCBI, defined as the fraction of the yellow pixels multiplied by 1000), the calcific burden index (CaBI, defined as the number of pixels indicating the presence of calcium, multiplied by 1000 and divided by the total number of pixels) and the $maxLCBI_{4mm}$ indicating the maximum LCBI in a 4-mm segment (Figure 2).

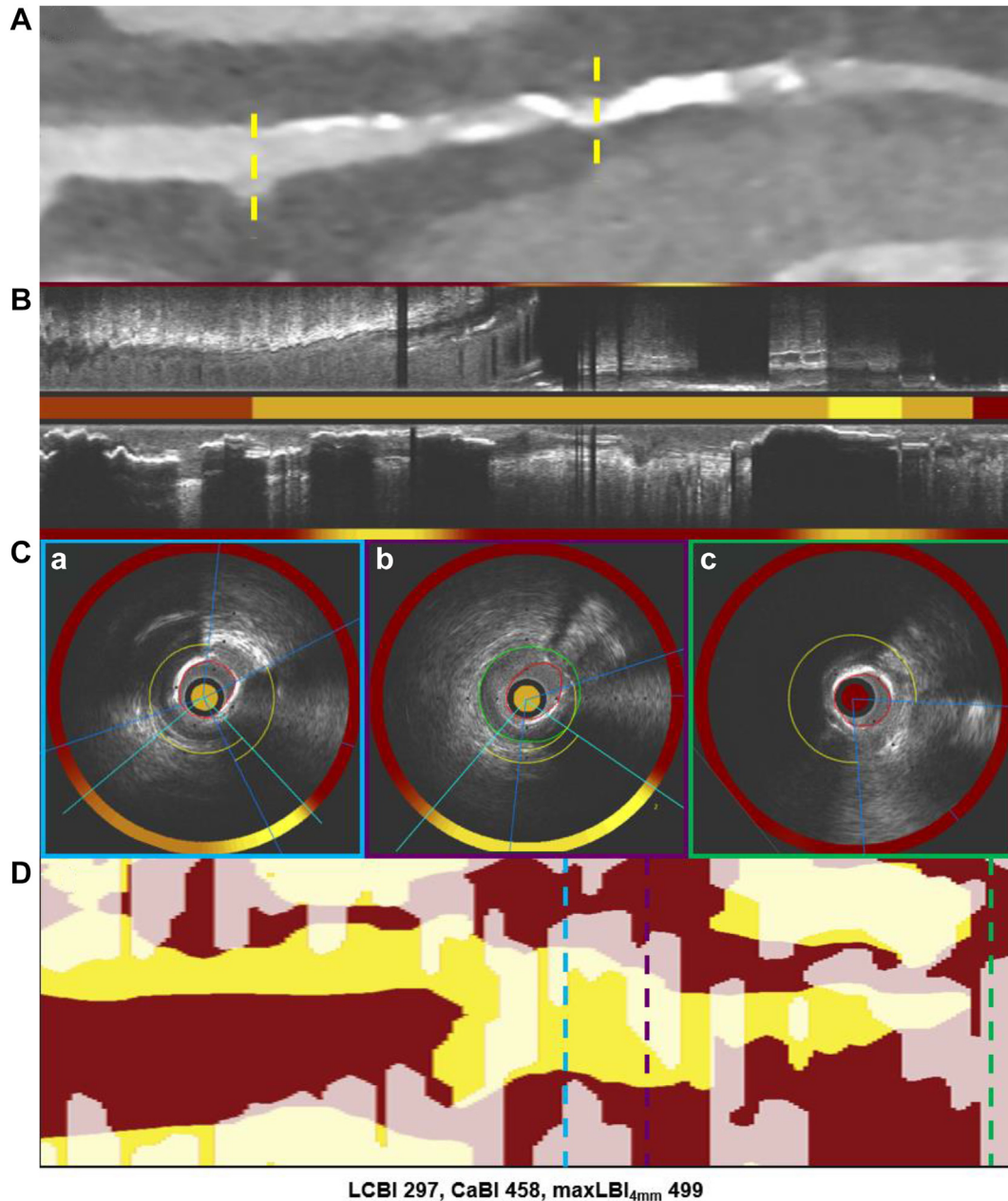LCBI 297, CaBI 458, $maxLBI_{4mm}$ 499

Figure 2.
A case example showing the methodology followed to examine the association of the coronary artery calcium score (CACS) and plaque morphology assessed by near-infrared spectroscopy-intravascular ultrasound (NIRS-IVUS). Panel (**A**) illustrates a multiplanar curve image of a left anterior descending coronary artery. The yellow dashed lines indicate the proximal and distal end of the segment of interest assessed by NIRS-IVUS. Panel (**B**) portrays a longitudinal NIRS-IVUS section of the segment of interest with the block chemogram shown in the middle of the panel, whereas (**C**)—(a), (b), and (c) illustrate NIRS-IVUS frames with the annotated lumen and external elastic membrane (EEM) borders. The circumferential extent of calcific tissue is indicated with a dark blue and of the necrotic core with light blue angles. Finally, panel (**D**) portrays a spread-out plot of plaque composition with the yellow color corresponding to lipid core tissue and the semitransparent white to calcific tissue. The green, purple, and blue dashed lines indicate the location of the NIRS-IVUS cross section in the spread-out plot. The lipid core burden index (LCBI), calcific burden index (CaBI), and $maxLCBI_{4mm}$ values for this segment are shown at the bottom of this panel.

Moreover, in each segment of interest, we detected the presence of lesions defined as 3 consecutive end-diastolic NIRS-IVUS frames with a plaque burden (defined as EEM–lumen area $\times$ 100 divided by the EEM area) >40%. If between lesions there was a disease-free segment with a length $\geq$5 mm, then these lesions were considered tandem lesions otherwise they were treated as a single lesion.[24] Previous studies have shown that lesions with a minimum lumen area $\leq$4 mm,[25] maximum plaque burden $\geq$70%,[25,26] and maxLCBI$_{4mm}$>400[26,27] are at risk of progressing and causing events. In the present analysis, the lesions that had all these 3 plaque characteristics were considered as high-risk lesions.

For each segment of interest, we examined the association between CACS and TAV, PAV, LCBI, CaBI, maxLCBI$_{4mm}$, and the number of lesions detected. In addition, we compared the CACS in segments with high-risk lesions and in those without.

Patient-level analysis. The lumen and EEM volume measured in the segments of interest were used to estimate the total lumen and EEM volume and extract the TAV and PAV for each patient. Moreover, we computed the LCBI, CaBI, and maxLCBI$_{4mm}$ and examined the association between the CACS estimated in the entire coronary tree of each patient with the above metrics. Finally, we reported the number of lesions detected by NIRS-IVUS and the presence of high-risk lesions and compared the CACS in patients with high-risk lesions with those without.

Statistical analysis

The Kolmogorov-Smirnov and Shapiro-Wilk tests were used to test the distribution of the numerical variables; for the normally distributed variables results are presented as mean and SD whereas for non-normally distributed variables as median and IQR; finally, categorical variables are shown as absolute values and percentages. The CACS was used to split the studied patients into terciles. ANOVA test was used to compare normally distributed variables, the Kruskal-Wallis test non-normally distributed variables, whereas the χ^2 test was applied for numerical variables.

Pearson for the normally distributed and Spearman correlation coefficient for the nonnormally distributed variables were used to examine the association between NIRS-IVUS–derived metrics and CACS, whereas binary logistic regression analysis was applied to investigate the association between the CACS and the incidence of high-risk lesions.

For segment-level analyses, mixed effects nested linear regression analyses were performed to examine the association between CACS and the following metrics: TAV, PAV, LCBI, CaBI, maxLCBI$_{4mm}$, lesion number, and presence of high-risk lesions, controlling for different vessel types within individual patients. This was expressed as coefficients with corresponding 95% CI. Given the nonparametric nature of all variables (except PAV), transformations were performed followed by an assessment of linearity between CACS and TAV, PAV, LCBI, CaBI, and maxLCBI$_{4mm}$. The choice of transformation was guided by the "gladder" command in Stata (output in Supplemental Figures S1 and S2). The CACS was log-transformed, whereas the TAV, LCBI, CaBI, and maxLCBI$_{4mm}$ were transformed to their square root. A P value of <.05 was considered statistically significant. Analysis was performed using the SPSS Statistic 26 (IBM) and Stata/MP 16 (StataCorp LLC).

Results

Studied patients

Of the 70 patients recruited in the study, 65 completed the studied protocol; all these patients had successful CACS assessment and were included in the analysis (Figure 3). The mean age of the recruited patients was 61.42 $\pm$ 8.22 years; most of the patients suffered from hypertension and hypercholesterolemia and had a positive family history of ischemic heart disease. The baseline demographics of the included patients are shown in Table 1.[2]

NIRS-IVUS imaging was successfully performed in 197 coronary arteries 11.4 $\pm$ 6.9 days after CTA; matching of the NIRS-IVUS and CTA images was possible in 188 segments, and these were included in the final analysis.

Association between CACS and plaque characteristics at the patient-level

The CACS computed in the studied patients (median, 52; IQR, 11-159) was used to split the patients into terciles (first group CACS < 23, second group CACS between 23 and 108, and third group CACS > 108). Patients with high CACS had a higher body mass index and incidence of hypertension but otherwise, there were no significant differences in the baseline demographics between groups (Table 1).

The total length of the segments studied by NIRS-IVUS imaging was 171.5 $\pm$ 69.4 mm per patient and was similar in the 3 groups. The length of the left circumflex-obtuse marginals studied by NIRS-IVUS was larger
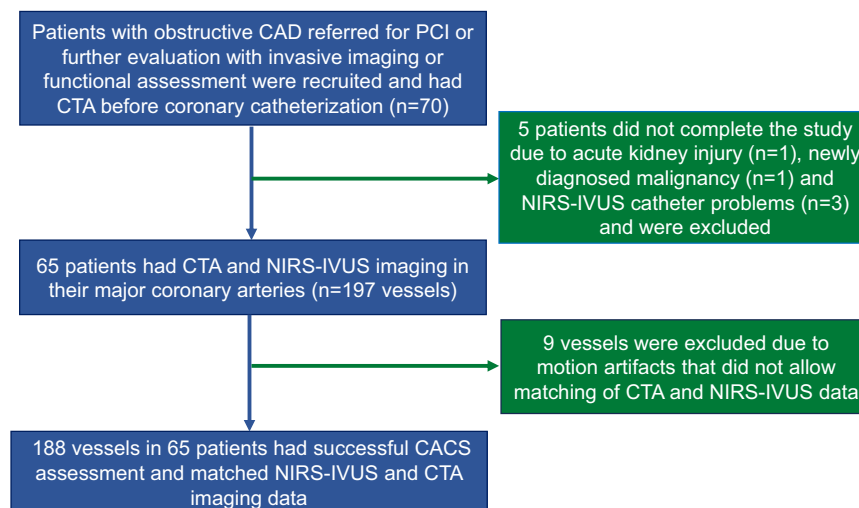

Figure 3.
Flowchart of study design. CACS, coronary artery calcium score; CAD, coronary artery disease; CTA, coronary computed tomography angiography; NIRS-IVUS, near-infrared spectroscopy-intravascular ultrasound; PCI, percutaneous coronary intervention.

Table 1. Baseline demographics of the studied patients in different CAC score terciles[a]

	Studied patients (N = 65)	Low CAC score tercile (n = 22)	Intermediate CAC score tercile (n = 22)	High CAC score tercile (n = 21)	P
Age, y	61.42 ± 8.22	59.29 ± 9.57	60.95 ± 7.59	64.05 ± 6.97	.164
Male sex	50 (76.9%)	14 (63.6%)	18 (81.8%)	18 (85.7%)	.183
BMI, kg/m²	28.1 [25.9-31.6]	26.2 [23.7-27.5]	29.7 [27.1-30.9]	31.2 [25.9-40.1]	.022
Smoking history	31 (47.7%)	11 (50%)	11 (50%)	9 (42.9%)	.865
Family history of CAD	40 (61.5%)	16 (72.7%)	14 (63.6%)	10 (47.6%)	.232
Comorbidities					
Hypertension	35 (53.8%)	11 (50%)	8 (36.4%)	16 (76.2%)	.035
Hypercholesterolemia	46 (70.8%)	17 (77.3%)	14 (63.6%)	15 (71.4%)	.608
Renal failure[a]	4 (6.15%)	2 (9.1%)	2 (9.1%)	0 (0%)	.373
Previous PCI	14 (21.5%)	3 (13.6%)	4 (18.2%)	7 (33.3%)	.261
Previous CVA	6 (9.2%)	2 (9.1%)	2 (9.1%)	2 (9.5%)	.998
LV dysfunction[b]	4 (6.2%)	1 (4.5%)	1 (4.5%)	2 (9.5%)	.737
Length of studied segments					
Total length, mm	171.5 ± 69.4	170.3 ± 52	179 ± 63	165 ± 64.6	.746
LAD—diagonals, mm	64.82 ± 32.10	62.78 ± 30.41	65.38 ± 39.45	66.38 ± 26.18	.932
LCx—obtuse marginals, mm	50.60 ± 28.16	62.20 ± 29.70	47.72 ± 22.05	41.45 ± 29.24	.043
RCA, mm	54.00 [0-96.43]	53.16 [0-81.17]	71.86 [0-105.35]	50.82 [0-10.23]	.359

Values are mean ± SD, n (%) or median [IQR].
CAD, coronary artery disease; CVA, cerebrovascular accident; LAD, left anterior descending artery; LCx, left circumflex coronary artery; LV, left ventricle; PCI, percutaneous coronary intervention; RCA, right coronary artery.
[a] Renal failure is defined as an estimated glomerular filtration rate of <60 mL/min/1.73 m². [b] LV dysfunction is defined as LV ejection fraction <50%.

in the intermediate CACS group but otherwise, there was no difference between groups in the length of vessels studied by NIRS-IVUS. The CACS analysis and the NIRS-IVUS analysis results are shown in Table 2. The lumen, EEM volume, TAV, and PAV as well as the LCBI and maxLCBI$_{4mm}$ were similar in the 3 groups, whereas the CaBI increased from the first to the third group. The median number of lesions detected in the segments studied by NIRS-IVUS was 4 (IQR, 3-6) and was no different in the 3 CACS categories. There was also no difference in the incidence of high-risk lesions in patients with low, intermediate, and high CACS (P = .628).

A weak correlation was noted between CACS and the PAV (r = 0.271; P = .002), whereas the correlation was moderate between the CACS and the CaBI (r = 0.648; P < .001). Conversely, there was no correlation between CACS and LCBI and maxLCBI$_{4mm}$. Binary logistic regression analysis did not demonstrate an association between CACS and the presence of high-risk lesions (P = .306).

Association of plaque composition and CAC at the segment level

The median length of the segments of interest was 54.79 (38.92-78.19). The mean CACS in these segments was 29.6 ± 68.0 and the

median CACS was 0 (0-120.0). The TAV estimated by NIRS-IVUS was 296 (150.0-469.5) mm³ and the PAV was 41.21% ± 9.89%. The LCBI was measured to be 38.27 (5.73-97.02), the CaBI 55.09 (16.59-119.97), and the maxLCBI$_{4mm}$ 261.15 (73.50-418.50). In total, 300 lesions were identified; the median number of lesions per segment was 1 (1-2) of which 25 (8.3%) were classified as high-risk lesions (only 1 segment had 2 high-risk lesions).

Linear regression analysis showed no association between segment-level log-transformed CACS and PAV, and root square LCBI and maxLCBI$_{4mm}$. Conversely, there was a significant association between the log-transformed CACS and the root-squared TAV and CaBI (Table 3, Figure 4). The number of lesions identified in the segments of interest, and the incidence of high-risk plaques, did not correlate with the CACS.

Reproducibility of CACS computation

An excellent agreement was noted between the estimations of the 2 analysts for the CACS measured in the entire coronary tree (ICC, 0.986; P < .001), and individually in each segment of interest assessed by NIRS-IVUS (ICC, 0.996; P < .001). Moreover, the reproducibility of the expert analyst who performed the analysis twice was also high and close

Table 2. CAC score and NIRS-IVUS analysis results in different CAC score terciles.

	Studied patients (N = 65)	Low CAC score tercile (n = 22)	Intermediate CAC score tercile (n = 22)	High CAC score tercile (n = 21)	P
CAC score					
Total CAC score	52 [11-159]	0 [0-11]	53 [38-80]	197 [165-408]	–
CAC score measured per patient in the segments of interest	34 [6-107]	0 [0-11]	44 [26-58]	166 [111-196]	–
NIRS-IVUS analysis					
Lumen volume, mm³	1404.3 ± 763.9	1298.7 ± 565.3	1565.5 ± 955.1	1346.2 ± 727.6	.474
EEM volume, mm³	2040.5 [1461.9-3130.4]	2093.8 [1452.3-2833.9]	2389.5 [1480-3169.1]	1866.9 [1461.9-3451.0]	.657
TAV, mm³	939.9 [591.6-1257.2]	794.0 [526.1-1145.6]	1010.1 [608.0-1447.6]	948.3 [591.6-1463.7]	.350
PAV, %	41.4 (8.43)	39.56 (9.20)	40.74 (7.52)	44.07 (8.21)	.194
LCBI	46.8 [20.6-88.8]	43.9 [23.4-65.3]	50.4 [17.3-88.8]	54.6 [32.4-106.8]	.724
CaBI	73.9 [37.5-120.1]	41.7 [21.7-64.0]	73.0 [38.5-114.7]	128.8 [109.6-205.8]	<.001
maxLCBI$_{4mm}$	455.6 ± 227.4	420.2 ± 181.3	444.6 ± 221.6	504.2 ± 274.6	.469
Number of lesions	4 [3-6]	4 [3-6]	5 [4-6]	5 [2-8]	.612
Presence of high-risk lesions	24 (36.9%)	9 (37.5%)	9 (37.5%)	6 (25.0%)	.628

Values are median [IQR], mean ± SD, or n (%).
CaBI, calcific burden index; CAC, coronary artery calcium; EEM, external elastic membrane; LCBI, lipid core burden index; PAV, percent atheroma volume; TAV, total atheroma volume.

Table 3. Association between coronary artery calcium score and plaque characteristics at the segment level.

	Coefficient	95% CI	P
TAV, mm^3	0.087	0.024 to 0.149	.008
PAV, %	0.087	−0.028 to 0.087	.309
CaBI	0.117	0.048 to 0.186	.001
LCBI	0.082	−0.007 to 0.170	.070
maxLCBI$_{4mm}$	0.030	−0.014 to 0.074	.169
Number of lesions detected by NIRS-IVUS	−0.084	−0.354 to 0.186	.537
Number of high-risk plaques	−0.233	−0.476 to 0.009	.059

CaBI, calcific burden index; LCBI, lipid core burden index; PAV, percent atheroma volume; TAV, total atheroma volume.

to 1 (ICC, 0.996; $P < .001$ for the CACS measured in the entire coronary artery tree, and ICC, 0.992; $P < .001$ for the CACS measured in the segments of interest).

Discussion

In this study, we examined for the first time in patients with established CAD the association between plaque characteristics assessed by NIRS-IVUS and CACS. We found that the CACS was weakly associated with the PAV and CaBI at the patient-level analysis and with the TAV and CaBI at the segment-level analysis. Conversely, in this cohort of patients, there was no association between the CACS and the lipid component assessed by NIRS or the incidence of high-risk lesions (Central Illustration).

Several studies in the past have demonstrated that the CACS provides useful prognostic information in asymptomatic individuals whereas in symptomatic patients the prognostic value of the CACS is less well established.[1–4,11,28] In the study by Mittal et al,[28] 0 CACS was associated with excellent clinical outcomes whereas in the study by Osborne-Grinter et al,[11] 10% of the patients who had an event at 4.8 years follow-up had 0 CACS at baseline. In the latter study, 13 of the patients with 0 CACS had CTA high-risk lesions with a large low attenuated plaque burden (>4%) that is a predictor of adverse events.[29] In this report, there was an association between CACS and plaque phenotypes with the patients having an increased CACS exhibiting more often low attenuated vulnerable plaques on CTA. Despite this association, however, plaque characteristics on CTA provided incremental prognostic information to CACS allowing better prediction of adverse events. These findings contradict a previous report that used NIRS-IVUS to assess plaque types and showed no association between plaque morphology and CACS and the results of Takamura et al[30] who failed to demonstrate a superiority of CTA over CACS in predicting outcomes.[12] A possible explanation of these discrepancies is the fact that these 2 analyses included asymptomatic patients who are less likely to have advanced plaque characteristics and also a small number of patients who may have not provided enough power to draw safe conclusions.

The present study overcomes the above limitations and for the first time it examined in a large number of symptomatic patients, with established CAD, the association between plaque morphology derived by hybrid NIRS-IVUS imaging and CACS. Similar to Madder et al,[12] we found a significant association between CACS, atheroma burden, and CaBI at the patient- and segment-level analysis. The association between the CACS and CaBI estimated by NIRS-IVUS was only moderate; this should be attributed to the fact that the CACS depends not only on the calcific area but also on calcium density and is traditionally estimated in CT sections obtained at a 3 mm interval, whereas, the CaBI reflects the longitudinal and circumferential extend of calcium in NIRS-IVUS and in our study was computed at every end-diastolic frame
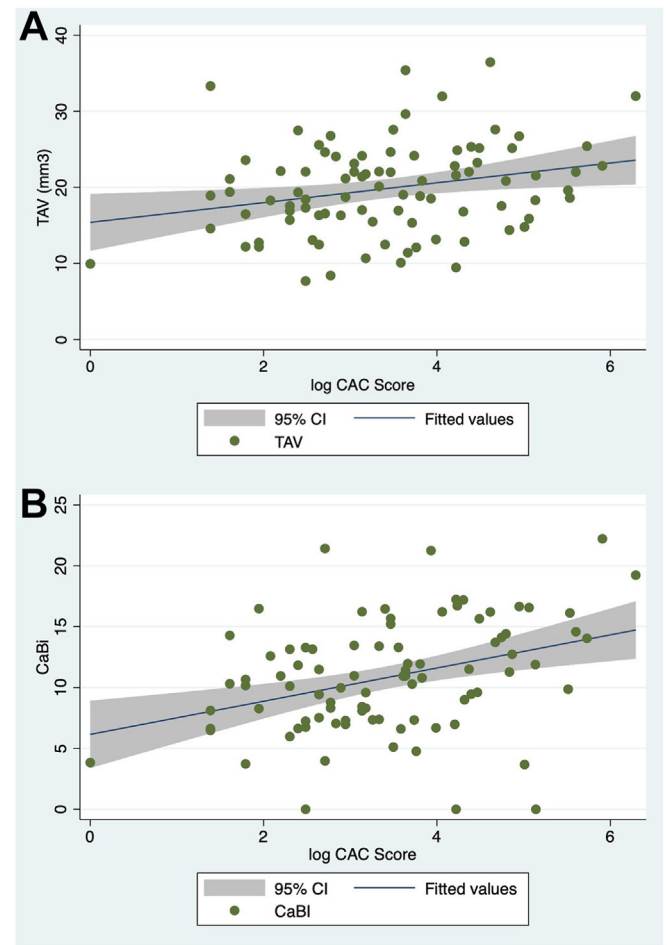

Figure 4.
Scatter plots showing the association between log-transformed coronary artery calcium score (CACS) and square root total atheroma volume (TAV) (A) and calcific burden index (CaBI) (B).

(average frame interval <0.5 mm). There is evidence that the difference in the longitudinal resolution between NIRS-IVUS and CACS affects their agreement for the calcific burden; in the study by Qian et al,[31] the CACS quantified in slices with a thickness of 0.5 mm had a better agreement with the calcific burden derived by IVUS than the conventional CACS measured in slices with a thickness of 3 mm. The large slice thickness may also have affected the association between CACS and lipid and plaque burden derived by NIRS-IVUS, especially in segments with short (<3 mm) lesions.[32] The weak correlation between atheroma burden and CACS noted in our analysis compared to the study Madder et al[12] should be also attributed to the different inclusion criteria of the 2 studies; our population included patients with 0 CACS that had advanced CAD, whereas the study by Madder et al[12] recruited patients with CACS of ≥300 who had less advanced disease, as indicated by the incidence of high-risk lesions in this population. Despite these differences, our findings were similar when we examined the association between the lipid component and CACS. In contrast to the study by Choi et al[13] that found a significant correlation between necrotic core computed by virtual histology-IVUS and CACS, in our analysis and in the analysis of Madder et al,[12] the lipid component detected by NIRS was not related to the CACS, which indicated that this modality may have limited predictive value in patients with advanced CAD. More importantly, CACS was not associated with the incidence of high-risk plaques identified by NIRS-IVUS imaging, as in our study 8 out of the 25 high-risk lesions were found in segments with 0 CACS; whereas, 1 in 5 patients with obstructive CAD had 0 CACS. The small number of
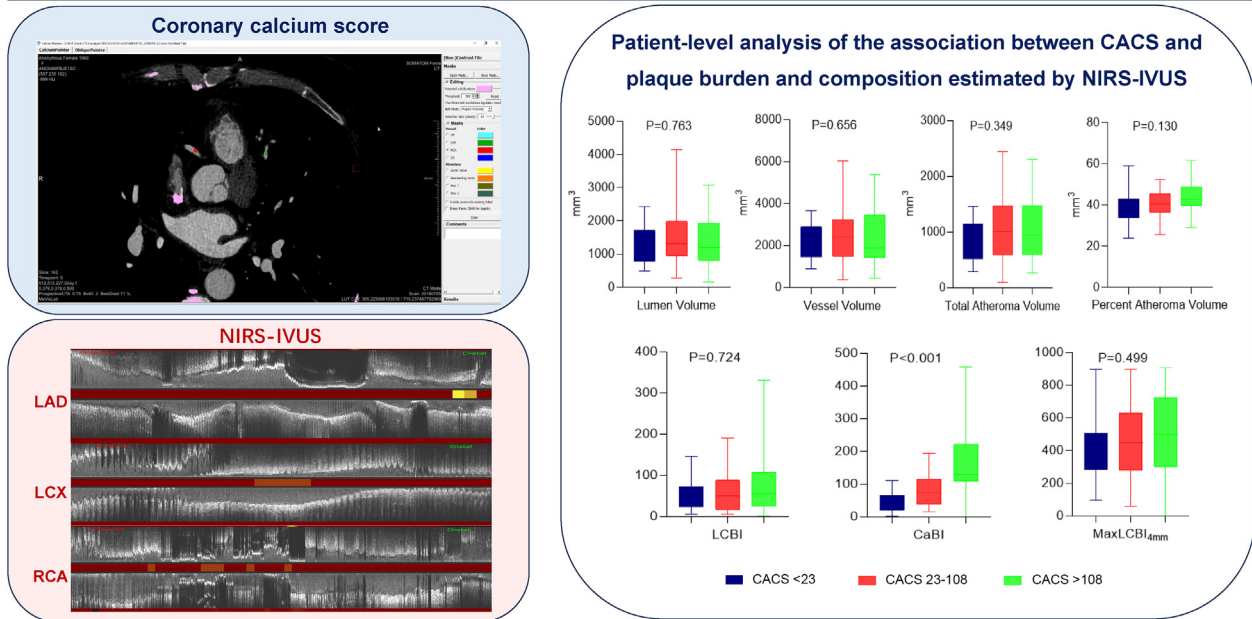
Central Illustration.
Association between coronary artery calcium score (CACS) and plaque characteristics detected by near-infrared spectroscopy-intravascular ultrasound (NIRS-IVUS).

patients in our analysis does not allow us to draw safe conclusions; however, it appears that CACS has limited efficacy in predicting plaque extension and morphology in patients with established CAD. This has also been shown in a previous study comparing CACS and plaque characteristics in patients with stable and acute coronary syndrome.[14] Therefore, in this setting, invasive or noninvasive imaging should be preferred for assessing plaque morphology, stratifying cardiovascular risk, and identifying vulnerable individuals who are likely to benefit from focal or systemic therapies targeting atherosclerosis. Considering the limited value of CACS to evaluate plaque morphology in our population, it can be hypothesized that CTA should be used instead of CACS as a screening tool in patients with a high probability of obstructive CAD as this enables comprehensive visualization of the coronary artery anatomy and detection of vulnerable lesions; this, however, needs to be proven by future large-scale clinical studies.

Limitations

Although this study is the largest report that examined the association between plaque morphology, derived by multimodality intravascular imaging and CACS, it has limitations that should be acknowledged. Firstly, the CACS was measured in contrast CTA using dedicated software and not in noncontrast CT that is conventionally used for this purpose. Noncontrast CT was not performed as per the study protocol to minimize the additional radiation associated with this test.[22] However, today there is convincing evidence that contrast CTA provides an effective alternative for the computation of the CACS as multiple studies have shown a small bias and narrow limits of agreement between the CACS estimated by CTA and noncontrast CT.[20,22,33] These evidences, the high reproducibility of the analysts, as well as the robust methodology implemented to compute the CACS that allowed use of the multiplanar images to ensure accurate calcific spot detection provide us confidence about the reported results. Secondly, this analysis included only patients who had obstructive CAD amenable to PCI as patients with advanced CAD, who usually have increased coronary calcification, and are referred for surgical revascularization, were excluded. It is unlikely, however, that this selection bias would have affected the main message of this analysis which was the high incidence of high-risk lesions in patients with 0 or very low CACS. Thirdly, the number of patients included was not sufficient to allow their classification in the CACS categories proposed by Rumberger et al[34] to compare the plaque composition in different CACS groups. Fourthly, in our cohort, only 25 high-risk lesions were detected, a number that did allow a detailed assessment of the association between plaque phenotypes and CACS. A lesion-level comparison of the CACS values in high- and low-risk lesions may have increased our sample size and allowed us to partially overcome this limitation[12,31,32]; however, the matching of the NIRS-IVUS and CT data at the lesion level was not possible with the CaclScore software. Finally, predilatation was performed in 6 cases as the NIRS-IVUS catheter could not cross these lesions. This is likely to have only a minimum effect on the estimated lumen, vessel, and PAV as in all occasions a 2 mm balloon was used for predilatation and it is unlikely to have affected the TAV computation as balloon dilatation does not reduce the plaque volume but causes dissection, plaque redistribution, and vessel enlargement.[35] Only 2 of the lesions that were predilated had a maxLCBI$_{4mm}$ >400 and a PB <70% post predilatation and were not considered as high-risk lesions; this classification, however, may have been different if NIRS-IVUS was possible without balloon dilatation.

Conclusions

Coronary artery calcium score is associated with atheroma burden but it has a limited value in predicting the lipid burden and the presence of high-risk lesions in patients with obstructive CAD. Our findings indicate that this modality may have a limited value as a screening tool and to stratify cardiovascular risk in symptomatic patients with multiple risk factors who have a high probability of suffering from obstructive CAD. Considering, however, the small number of recruited patients and the selection bias, further research is needed in this direction and the conduction of large-scale analysis before drawing firm conclusions.

Declaration of competing interest

Funding sources

Ethics statement and patient consent

The reported research has adhered to the relevant ethical guidelines; patient consent has been obtained from all the included patients.

Supplementary material

To access the supplementary material accompanying this article, visit the online version of the *Journal of the Society for Cardiovascular Angiography & Interventions* at 10.1016/j.jscai.2024.101308.

References

1. Javaid A, Mitchell JD, Villines TC. Predictors of coronary artery calcium and long-term risks of death, myocardial infarction, and stroke in young adults. *J Am Heart Assoc*. 2021;10(22):e022513. https://doi.org/10.1161/JAHA.121.022513
2. Lehmann N, Erbel R, Mahabadi AA, et al. Value of progression of coronary artery calcification for risk prediction of coronary and cardiovascular events: result of the HNR study (Heinz Nixdorf recall). *Circulation*. 2018;137(7):665–679. https://doi.org/10.1161/CIRCULATIONAHA.116.027034
3. Budoff M, Backlund JC, Bluemke DA, et al. The association of coronary artery calcification with subsequent incidence of cardiovascular disease in type 1 diabetes: the DCCT/EDIC trials. *JACC Cardiovasc Imaging*. 2019;12(7 Pt 2): 1341–1349. https://doi.org/10.1016/j.jcmg.2019.01.014
4. Carr JJ, Jacobs DR Jr, Terry JG, et al. Association of coronary artery calcium in adults aged 32 to 46 years with incident coronary heart disease and death. *JAMA Cardiol*. 2017;2(4):391–399. https://doi.org/10.1001/jamacardio.2016.5493
5. Visseren FLJ, Mach F, Smulders YM, et al. 2021 ESC Guidelines on cardiovascular disease prevention in clinical practice. *Eur Heart J*. 2021;42(34):3227–3337. https://doi.org/10.1093/eurheartj/ehab484
6. Coylewright M, Rice K, Budoff MJ, et al. Differentiation of severe coronary artery calcification in the Multi-Ethnic Study of Atherosclerosis. *Atherosclerosis*. 2011; 219(2):616–622. https://doi.org/10.1016/j.atherosclerosis.2011.08.038
7. Peng AW, Mirbolouk M, Orimoloye OA, et al. Long-term all-cause and cause-specific mortality in asymptomatic patients with CAC ≥1,000: results from the CAC consortium. *JACC Cardiovasc Imaging*. 2020;13(1 Pt 1):83–93. https://doi.org/10.1016/j.jcmg.2019.02.005
8. Peng AW, Dardari ZA, Blumenthal RS, et al. Very high coronary artery calcium (≥1000) and association with cardiovascular disease events, non-cardiovascular disease outcomes, and mortality: results from MESA. *Circulation*. 2021;143(16): 1571–1583. https://doi.org/10.1161/CIRCULATIONAHA.120.050545
9. Shaw LJ, Giambrone AE, Blaha MJ, et al. Long-term prognosis after coronary artery calcification testing in asymptomatic patients: a cohort study. *Ann Intern Med*. 2015; 163(1):14–21. https://doi.org/10.7326/M14-0612
10. Budoff MJ, Shaw LJ, Liu ST, et al. Long-term prognosis associated with coronary calcification: observations from a registry of 25,253 patients. *J Am Coll Cardiol*. 2007;49(18):1860–1870. https://doi.org/10.1016/j.jacc.2006.10.079
11. Osborne-Grinter M, Kwiecinski J, Doris M, et al. Association of coronary artery calcium score with qualitatively and quantitatively assessed adverse plaque on coronary CT angiography in the SCOT-HEART trial. *Eur Heart J Cardiovasc Imaging*. 2022;23(9):1210–1221. https://doi.org/10.1093/ehjci/jeab135
12. Madder RD, VanOosterhout S, Klungle D, et al. Multimodality intracoronary imaging with near-infrared spectroscopy and intravascular ultrasound in asymptomatic individuals with high calcium scores. *Circ Cardiovasc Imaging*. 2017;10(10). https://doi.org/10.1161/CIRCIMAGING.117.006282
13. Choi YH, Hong YJ, Park IH, et al. Relationship between coronary artery calcium score by multidetector computed tomography and plaque components by virtual histology intravascular ultrasound. *J Korean Med Sci*. 2011;26(8):1052–1060. https://doi.org/10.3346/jkms.2011.26.8.1052
14. van Velzen JE, de Graaf FR, Jukema JW, et al. Comparison of the relation between the calcium score and plaque characteristics in patients with acute coronary syndrome versus patients with stable coronary artery disease, assessed by computed tomography angiography and virtual histology intravascular ultrasound. *Am J Cardiol*. 2011;108(5):658–664. https://doi.org/10.1016/j.amjcard.2011.04.009
15. Ramasamy A, Safi H, Moon JC, et al. Evaluation of the efficacy of computed tomographic coronary angiography in assessing coronary artery morphology and physiology: rationale and study design. *Cardiology*. 2020;145(5):285–293. https://doi.org/10.1159/000506537
16. Bajaj R, Huang X, Kilic Y, et al. Advanced deep learning methodology for accurate, real-time segmentation of high-resolution intravascular ultrasound images. *Int J Cardiol*. 2021;339:185–191. https://doi.org/10.1016/j.ijcard.2021.06.030
17. Bajaj R, Huang X, Kilic Y, et al. A deep learning methodology for the automated detection of end-diastolic frames in intravascular ultrasound images. *Int J Cardiovasc Imaging*. 2021;37(6):1825–1837. https://doi.org/10.1007/s10554-021-02162-x
18. Keelan PC, Bielak LF, Ashai K, et al. Long-term prognostic value of coronary calcification detected by electron-beam computed tomography in patients undergoing coronary angiography. *Circulation*. 2001;104(4):412–417. https://doi.org/10.1161/hc2901.093112
19. Hong C, Becker CR, Schoepf UJ, Ohnesorge B, Bruening R, Reiser MF. Coronary artery calcium: absolute quantification in nonenhanced and contrast-enhanced multi-detector row CT studies. *Radiology*. 2002;223(2):474–480. https://doi.org/10.1148/radiol.2232010919
20. van der Bijl N, Joemai RM, Geleijns J, et al. Assessment of Agatston coronary artery calcium score using contrast-enhanced CT coronary angiography. *AJR Am J Roentgenol*. 2010;195(6):1299–1305. https://doi.org/10.2214/AJR.09.3734
21. Mühlenbruch G, Wildberger JE, Koos R, et al. Coronary calcium scoring using 16-row multislice computed tomography: nonenhanced versus contrast-enhanced studies in vitro and in vivo. *Invest Radiol*. 2005;40(3):148–154. https://doi.org/10.1097/01.rli.0000153024.12712.10
22. Ahmed W, de Graaf MA, Broersen A, et al. Automatic detection and quantification of the Agatston coronary artery calcium score on contrast computed tomography angiography. *Int J Cardiovasc Imaging*. 2015;31(1):151–161. https://doi.org/10.1007/s10554-014-0519-4
23. Glodny B, Helmel B, Trieb T, et al. A method for calcium quantification by means of CT coronary angiography using 64-multidetector CT: very high correlation with Agatston and volume scores. *Eur Radiol*. 2009;19(7):1661–1668. https://doi.org/10.1007/s00330-009-1345-2
24. García-García HM, Gomez-Lara J, Gonzalo N, et al. A comparison of the distribution of necrotic core in bifurcation and non-bifurcation coronary lesions: an in vivo assessment using intravascular ultrasound radiofrequency data analysis. *EuroIntervention*. 2010;6(3):321–327. https://doi.org/10.4244/EIJV6I3A54
25. Stone GW, Maehara A, Lansky AJ, et al. A prospective natural-history study of coronary atherosclerosis. *N Engl J Med*. 2011;364(3):226–235. https://doi.org/10.1056/NEJMoa1002358
26. Erlinge D, Maehara A, Ben-Yehuda O, et al. Identification of vulnerable plaques and patients by intracoronary near-infrared spectroscopy and ultrasound (Prospect II): a prospective natural history study. *Lancet*. 2021;397(10278):985–995. https://doi.org/10.1016/S0140-6736(21)00249-X
27. Waksman R, Di Mario C, Torguson R, et al. Identification of patients and plaques vulnerable to future coronary events with near-infrared spectroscopy intravascular ultrasound imaging: a prospective, cohort study. *Lancet*. 2019;394(10209): 1629–1637. https://doi.org/10.1016/S0140-6736(19)31794-5
28. Mittal TK, Pottle A, Nicol E, et al. Prevalence of obstructive coronary artery disease and prognosis in patients with stable symptoms and a zero-coronary calcium score. *Eur Heart J Cardiovasc Imaging*. 2017;18(8):922–929. https://doi.org/10.1093/ehjci/jex037
29. Williams MC, Kwiecinski J, Doris M, et al. Low-attenuation noncalcified plaque on coronary computed tomography angiography predicts myocardial infarction: results from the multicenter SCOT-HEART trial (Scottish computed tomography of the HEART). *Circulation*. 2020;141(18):1452–1462. https://doi.org/10.1161/CIRCULATIONAHA.119.044720
30. Takamura K, Fujimoto S, Kondo T, et al. Incremental prognostic value of coronary computed tomography angiography: high-risk plaque characteristics in asymptomatic patients. *J Atheroscler Thromb*. 2017;24(11):1174–1185. https://doi.org/10.5551/jat.39115
31. Qian Z, Dhungel A, Vazquez G, Weeks M, Voros S, Rinehart S. Coronary artery calcium: 0.5-mm slice-thickness reconstruction with adjusted attenuation threshold outperforms 3.0 mm by validating against spatially registered intravascular ultrasound with radiofrequency backscatter. *Acad Radiol*. 2015;22(9): 1128–1137. https://doi.org/10.1016/j.acra.2015.03.016
32. Okabe T, Mintz GS, Weigold WG, et al. The predictive value of computed tomography calcium scores: a comparison with quantitative volumetric intravascular ultrasound. *Cardiovasc Revasc Med*. 2009;10(1):30–35. https://doi.org/10.1016/j.carrev.2008.07.001
33. Bischoff B, Kantert C, Meyer T, et al. Cardiovascular risk assessment based on the quantification of coronary calcium in contrast-enhanced coronary computed tomography angiography. *Eur Heart J Cardiovasc Imaging*. 2012;13(6):468–475. https://doi.org/10.1093/ejechocard/jer261
34. Rumberger JA, Brundage BH, Rader DJ, Kondos G. Electron beam computed tomographic coronary calcium scanning: a review and guidelines for use in asymptomatic persons. *Mayo Clin Proc*. 1999;74(3):243–252. https://doi.org/10.4065/74.3.243
35. Mintz GS, Pichard AD, Kent KM, Satler LF, Popma JJ, Leon MB. Axial plaque redistribution as a mechanism of percutaneous transluminal coronary angioplasty. *Am J Cardiol*. 1996;77(5):427–430. https://doi.org/10.1016/s0002-9149(97)89379-4